COMPUTER SIMULATION OF ULTRASONIC WAVES IN SOLIDS

GORDON A. THIBAULT
Professional Experience Year Student
University of Toronto

and

KEN CHAPLIN
Non-Destructive Testing Development Branch
AECL Research

ABSTRACT

A computer model that simulates the propagation of ultrasonic waves has been developed at AECL Research, Chalk River Laboratories. This program is called EWE, short for Elastic Wave Equations, the mathematics governing the propagation of ultrasonic waves. This report contains: a brief summary of the use of ultrasonic waves in non-destructive testing techniques, a discussion of the EWE simulation code explaining the implementation of the equations and the types of output received from the model, and an example simulation showing the abilities of the model.

1. Use of Ultrasonics in Non-Destructive Testing

Ultrasonic waves are used in the non-destructive testing of materials to discover any defects or discontinuities inside the material. This is achieved by creating a wave using a piezoelectric transducer, which converts an electrical signal to an oscillating pressure with a frequency in the megahertz range. This wave travels through the material, interacting with any defects or discontinuities in its path, and is then received by either the same transducer, or a transducer in a different location. The signal is then converted back to electrical energy, and is displayed as an amplitude or A-scan, which is a graph of the electrical signal as a function of time.

2. EWE (Elastic Wave Equations)

2.1 *Explanation of the Equations and Their Implementation*

The EWE model was designed to perform all the operations of a real ultrasonic test. To explain how this is accomplished, here are the Elastic Wave Equations calculated by the model:

$$\rho \frac{\partial \dot{u}}{\partial t} = \frac{\partial X_x}{\partial x} + \frac{\partial X_y}{\partial y} \tag{2.1}$$

$$\rho \frac{\partial \dot{v}}{\partial t} = \frac{\partial X_y}{\partial x} + \frac{\partial Y_y}{\partial y} \tag{2.2}$$

$$\frac{\partial X_x}{\partial t} = (\lambda+2\mu)\frac{\partial \dot{u}}{\partial x} + \lambda \frac{\partial \dot{v}}{\partial y} \tag{2.3}$$

$$\frac{\partial Y_y}{\partial t} = (\lambda+2\mu)\frac{\partial \dot{v}}{\partial y} + \lambda \frac{\partial \dot{u}}{\partial x} \tag{2.4}$$

$$\frac{\partial X_y}{\partial t} = \mu \frac{\partial \dot{u}}{\partial y} + \mu \frac{\partial \dot{v}}{\partial x} \tag{2.5}$$

where $\dot{u}$ and $\dot{v}$ are velocities, and X_x, X_y, Y_x, and Y_y are stresses. These equations hold true for an isotropic, uniform medium. Note that in (2.1) and (2.2), the derivatives of the velocities $\dot{u}$ and $\dot{v}$ depend on the derivatives of the stresses X_x, X_y, and Y_y, and in (2.3), (2.4) and (2.5), the derivatives of the stresses X_x, X_y, and Y_y depend on the derivatives of the velocities $\dot{u}$ and $\dot{v}$. Using these equations, two grids are established containing velocity and stress data. These grids then interpenetrate in space to form the given region. Velocities are calculated at grid points from stresses on surrounding grid points. Similarly, the stress grid is calculated to find the new velocity grid. This repeats to propagate the wave through the grids. Additional formulas are used to calculate velocity and stress data for cracks, slots, and absorbing or reflecting boundaries. Data is also collected at the surface closest to the transducer, over the time period of the simulation, to allow the calculation of the signal displayed in an A-scan.

2.2 *Output Types From the Model*

These calculations generate considerable amounts of data. A realistic simulation produces files on the order of 250MB, and could take 24 hours of CPU time to execute on the Cyber 990 mainframe. To analyze these results, graphical visualization techniques are implemented. The data files consist of values of $\dot{u}$ and $\dot{v}$ for the region stored at several regular time intervals. The data is then put into a commercially-provided graphics package available on the Cyber, such as CA-DISSPLA or NCAR. These packages create contour plots of the data to show the waves. The output capabilities of the model include:

- Energy Displays; created from the velocity data, displayed in Fig. 1.
- Compression Wave Velocity Displays; created by employing a DIV operator on the wave fields, which attenuates the shear waves.
- Shear Wave Velocity Displays; created by employing a CURL operator on the wave fields, which attenuates the compression waves.
- Vector Displays; created from the velocity data.
- Focal Point Displays; created from the maximum energy at each point over the duration of the simulation.
- A-Scan graphs; similar to experimental data from ultrasonic instruments.

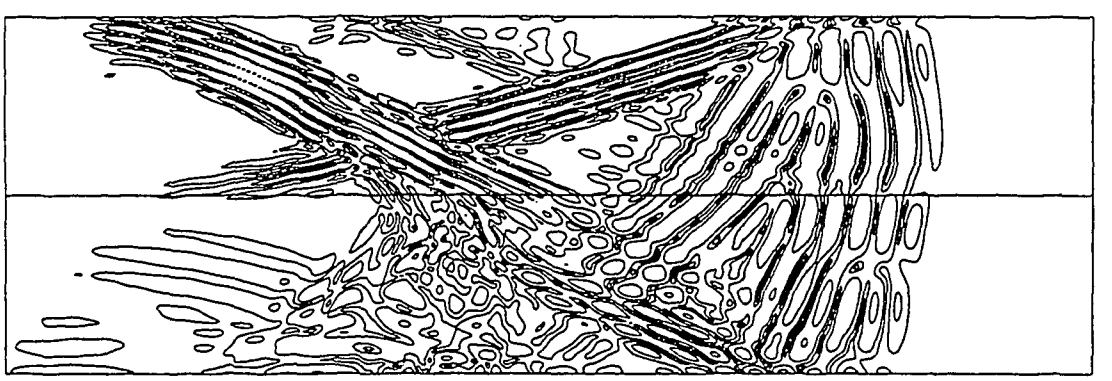

Fig. 1 Energy Display output from the EWE model. The waves with large wavelengths are compression waves, and the small wavelength waves are shear waves.

There are some capabilities to produce colour contour displays, and animated simulation is among our present endeavors. All these tools are useful in analyzing the interaction of ultrasonic waves with defects and discontinuities, and in interpretation of inspection results such as an A-scan.

3. Application Example

Materials have a property known as a critical angle, which represents the angle of total internal reflection. This means that if a wave hits a boundary at an angle below the critical angle, it will split into different types of waves and divide its energy among these new waves. This division process is called mode conversion. If a waves hits a boundary above the critical angle, it will completely reflect from the boundary.

Through a previous simulation, an interesting effect was observed. When a shear wave hit the backwall surface at just below the critical angle of the material, some energy is mode converted into a compression wave travelling parallel to the surface. This compression wave then mode converted back to a shear wave at the backwall surface, and travelled along side the original shear wave, which reflected the rest of the energy.

We decided to see if this phenomena occured in real materials, so we tried this technique using zirconium as the material. In zirconium, the critical angle is 29°, so we chose a smaller angle of 26°, and ran the simulation. It exhibited many of the same effects as the first simulation, except more energy converted to compression wave, therefore there was a significant drop in amplitude of the shear wave upon reflection. Through the study of this case, it was hypothesized that if a layer of material with a critical angle of less than 26° was placed inside the backwall surface of the zirconium, the shear wave would not mode convert to compression wave. It would just reflect off the backwall surface entirely. Such a material did exist in zirconium hydride, a material found in blister defects on pressure tubes. Zirconium hydride has a critical angle of about 20°.

We ran the new simulation with a zirconium hydride layer in place. As predicted, most of the energy did reflect back from the boundary. A comparison between the plain zirconium and the zirconium hydride layer case was performed to see the effect on the amplitude of the reflected shear wave in detail. This was done by moving the receive transducer along the near surface of the region and finding the amplitude of the wave for each position. In a few spots, the shear wave was three times larger in the zirconium hydride than the plain zirconium. Another wave exhibited different effects in the two cases. This wave is caused partially by a compression wave converting to shear wave at the backwall surface, and partially by the initial shear wave converting to a compression wave at the backwall surface. Both these waves meet the near surface of the region at the same time, creating a single wave. Its amplitude decreased slightly in the zirconium hydride case compared to the zirconium case.

Since in the zirconium case, this compression-shear wave was about half the size of the shear wave, simple mathematical manipulation of the signals could be used to give a result that is near zero for the case of pure zirconium, and large for a case with zirconium hydride. By subtracting twice the amplitude of the compression-shear wave from the amplitude of the shear-shear wave, this effect is realized. The zirconium hydride signal is 10 times the size of the zirconium signal using this method, as shown in Fig. 2.

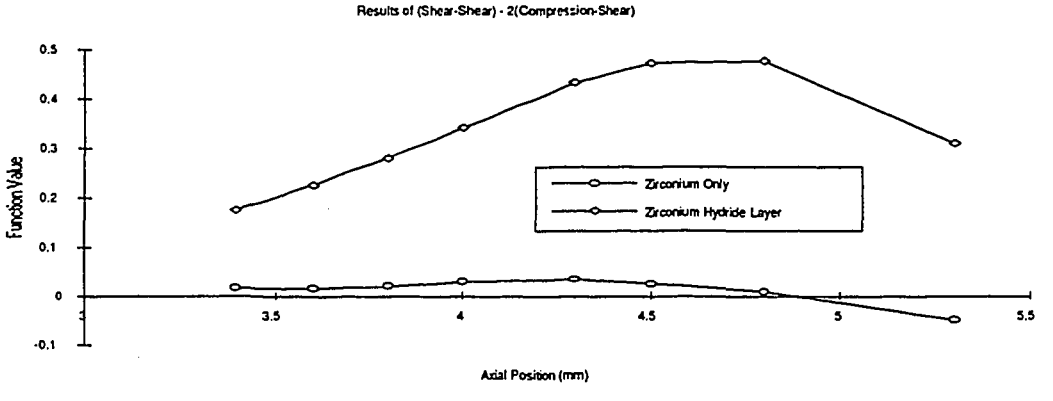

Fig. 2 Graph of possible function to improve detection of zirconium hydride .

All the ideas for this example were triggered and analyzed by simulation with the computer model. In this way, we hope to be able to develop new techniques for inspection, as well as further understanding and explanation of existing inspection results.

Acknowledgements

The support of COG, WP#34, WPIR 6542 for this work is gratefully acknowledged.

Bibliography

1. S.R. Douglas and K.R. Chaplin, *EWE: A Computer Model for Ultrasonic Inspection*, AECL-10507/COG 91-261.
2. K.R. Chaplin, S.R. Douglas, A.W. Leung, and G.A. Thibault, 1992, *unpublished report.*